International Journal of Pharmaceutics 397 (2010) 84–91

Contents lists available at ScienceDirect

International Journal of Pharmaceutics

journal homepage: www.elsevier.com/locate/ijpharm

Potential of amorphous microporous silica for ibuprofen controlled release

C.A. Aerts[a], E. Verraedt[a], A. Depla[a], L. Follens[a], L. Froyen[c], J. Van Humbeeck[c], P. Augustijns[b], G. Van den Mooter[b], R. Mellaerts[a], J.A. Martens[a,*]

[a] Centre for Surface Chemistry and Catalysis, K.U. Leuven, Kasteelpark Arenberg 23, 3001 Leuven, Belgium
[b] Laboratory for Pharmacotechnology and Biopharmacy, K.U. Leuven, Herestraat 49, Bus 921, 3000 Leuven, Belgium
[c] Department of Metallurgy and Materials Engineering, K.U. Leuven, Kasteelpark Arenberg 44, 3001 Leuven, Belgium

ARTICLE INFO

Article history:
Received 5 May 2010
Received in revised form 24 June 2010
Accepted 30 June 2010
Available online 7 July 2010

Keywords:
Sol–gel
Silica
Ibuprofen
Controlled release
Micropore diffusion

ABSTRACT

Amorphous microporous silica (AMS) xerogel materials were synthesized in an acid-catalyzed sol–gel process. The porosity of AMS was adapted by varying sol–gel synthesis parameters including the molar hydrolysis ratio (*r*-value), HCl:Si molar ratio, the type of silicon alkoxide source and the solvent. AMS particles of millimeter size were loaded with ibuprofen, by heat treatment and melt impregnation. *In vitro* release experiments were performed in simulated gastric and intestinal fluid. The release kinetics were critically depending on the AMS particle size distribution and the micropore diameter. The release was interpreted as configurational diffusion in the AMS micropores. The stability of unloaded and ibuprofen loaded AMS material upon storage was investigated using nitrogen physisorption, DSC analysis and *in vitro* release experiments. Ibuprofen loaded AMS formulations show remarkable stability, which can be attributed to the presence of ibuprofen molecules in the channels, functioning as scaffolds to support the pore structure.

1. Introduction

Silica is known for its excellent adsorptive properties and its ability to immobilize molecules with various functionalities inside pores. Derivatization of ordered mesoporous silica with active molecules is e.g. a means of developing molecular machines (Angelos et al., 2007). In the field of formulation of therapeutic drug compounds, ordered mesoporous silica materials are reservoirs for therapeutic compounds from which, depending on the pore width and dimensionality, molecules can be released either immediately (Mellaerts et al., 2007; Heikkila et al., 2007) or over a longer time frame through pore diffusion (Vallet-Regi et al., 2000; Munoz et al., 2002; Lai et al., 2003; Charnay et al., 2004; Horcajada et al., 2004, 2006b; Doadrio et al., 2004; Zeng et al., 2005; Izquierdo-Barba et al., 2005). Drug release can be fine-tuned by chemical functionalization of the mesopore wall (Munoz et al., 2002; Zeng et al., 2005; Izquierdo-Barba et al., 2005; Horcajada et al., 2006b), by adjusting the pore diameter, or by providing nanocaps for controlling the timing of the drug release (Lai et al., 2003). Drug molecules incorporated during sol–gel processing can be released by a combination of bio-erosion and pore diffusion (Santos et al., 1999; Kortesuo et al., 1999, 2000a,b, 2001a,b; Ahola et al., 2000, 2001; Czuryszkiewicz et al., 2002). Microporous silica materials present attractive controlled release properties as well. Crystalline microporous silicate materials were shown to be convenient carrier materials for delayed release of ibuprofen (Horcajada et al., 2006a). Recently, we demonstrated that configurational diffusion of ibuprofen can be realized in amorphous microporous silica (AMS) materials. AMS is a convenient microporous carrier to achieve a sustained diffusive release of a therapeutic drug molecule (Aerts et al., 2007) and an antiseptic (Verraedt et al., 2010).

Amorphous microporous silica, titania, zirconia, alumina and mixed metal oxides with a narrow pore size distribution can be synthesized in the absence of organic templates (Maier et al., 1993; Frenzer and Maier, 2006). These materials are obtained under acid-catalyzed sol–gel conditions at low water content. Under conditions with shortage of water (low *r*-value, referring in sol–gel literature to water:alkoxide molar ratio), the hydrolysis of the alkoxide source is incomplete. Linear chain growth is favored under such conditions (Brinker, 1988; Brinker and Scherer, 1990; Ro and In, 1991; Maier et al., 1993). The final gel contains residual alkoxy groups, which can be eliminated through calcination, whereupon a microporous material is obtained (Ro and In, 1991; Maier et al., 1993). Amorphous microporous mixed oxides have surface areas and porosities comparable to those of zeolites. Such materials can be used for the shape selective catalysis of hydrogenation and dehydrogenation reactions (Li et al., 2000), selective oxidation reactions with atmospheric oxygen, hydrogen peroxide or organic peroxides (Konietzni et al., 1998, 1999; Oresek et al., 1999; Stöckmann et al., 2001; Deng et al., 2001), isomerization reactions, esterification,

* Corresponding author. Tel.: +32 16 321610; fax: +32 16 321998.
E-mail address: johan.martens@biw.kuleuven.be (J.A. Martens).

0378-5173/$ – see front matter © 2010 Elsevier B.V. All rights reserved.
doi:10.1016/j.ijpharm.2010.06.053

etherification (Storck et al., 1997) and hydrocracking (Grimm et al., 1998).

Therapeutic drug molecules such as ibuprofen can be loaded on AMS by melting, impregnation or by adsorption from solution (Aerts et al., 2007). The ibuprofen diffusion coefficient in AMS at 37 °C varies from 10^{-11} to 10^{-14} m^2 s^{-1} depending on the micropore diameter (Aerts et al., 2007).

In this study, we investigated the stability of an AMS material with different porosity obtained by adapting the synthesis conditions. The impact of storage under dry and ambient conditions on the textural parameters and release performance was investigated.

2. Materials and methods

2.1. Synthesis of AMS

Amorphous microporous silica materials were prepared according to Maier et al. by combining silicon alkoxide, solvent and HCl (37%, Chem-lab, Zedelgem, Belgium) (Maier et al., 1993). Tetraethylorthosilicate (TEOS, 98%, Acros, Geel, Belgium) and tetramethylorthosilicate (TMOS, 99%, Acros, Geel, Belgium) were used as silicon alkoxide source. The solvent in the sol–gel process was technical ethanol or methanol (HPLC grade, Acros, Geel, Belgium). The HCl:Si molar ratio and *r*-value in the silica sol ranged between 0.12–1.74 and 1.2–6, respectively. The code names of the AMS materials according to the sol–gel synthesis parameters are listed in Table 1. The AMS synthesis procedure was as follows. HCl was combined with water and added dropwise to the stirred solution of TEOS and ethanol. Stirring was continued for 24 h at room temperature. Subsequently, the sol was heated at 50 °C under quiescent conditions in a furnace for 3 days. A stiff transparent gel was obtained. The gel body was broken and the particles were heated to 65 °C with a heating ramp of 0.1 °C min^{-1}. After 5 h at 65 °C the material was heated to the final temperature of 250 °C with a slope of 0.1 °C min^{-1}. After 5 h at 250 °C, the product was cooled to ambient temperature. Finally, the xerogel was manually crushed using a mortar and pestle and subsequently sieved to different particle sizes.

2.2. Ibuprofen loading and in vitro release experiments

Ibuprofen (Alpha Pharma, Belgium) was loaded into AMS using the melting method. A physical mixture of AMS and ibuprofen powder was heated in a furnace at 100 °C for 24 h, which is above the ibuprofen melting temperature (75 °C). The standard ibuprofen loading was 10 wt.%. In order to study the release of the drug substance in a medium simulating the gastrointestinal tract, ibuprofen loaded AMS materials were dispersed in 1000 ml simulated gastric fluid (SGF, pH 1.2, USP XXV) at 37 °C under gentle agitation using a Hanson SR8-plusTM dissolution bath (USA). After 2 h, K_2HPO_4 (Merck, Overijse, Belgium) was added until the pH of the solution was 6.8, simulating human intestinal fluid.

2.3. Methods

Nitrogen adsorption isotherms at −196 °C were recorded on a Tristar instrument (Micromeritics, USA). Before the measurements, samples were outgassed for 12 h at 250 °C. Specific surface area and pore volume were determined using BET and *t*-plot analysis, respectively. The low pressure range ($10^{-7} < P/P_0 < 10^{-4}$) of the nitrogen adsorption isotherm was investigated on an ASAP 2020 instrument (Micromeritics, USA). The isotherms were interpreted in terms of micropore diameters using the Horvath-Kawazoe method for slit shaped pores (Horvath and Kawazoe, 1983).

The particle size of AMS materials was measured using a Mastersizer Micro Plus apparatus (Malvern Instruments, USA) by means of the Fraunhofer laser diffraction theory. The particles were suspended in ethanol during analysis. The measurement range of the Mastersizer is between 0.05 and 555 μm. The particle size distribution of larger AMS grains with a mean particle size of 800 μm was obtained by measuring the size of the grains using a stereoscope.

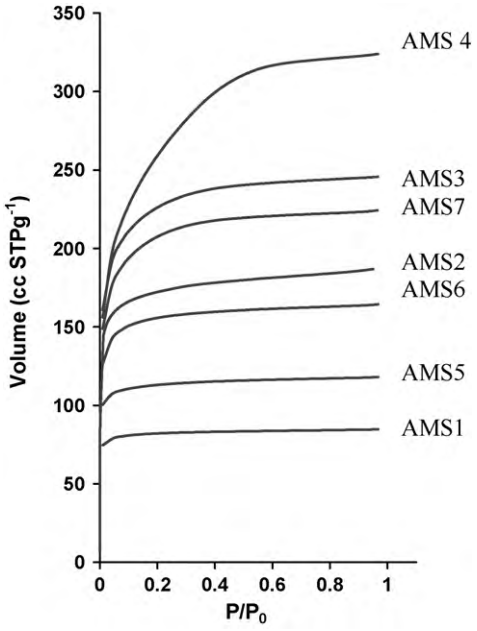

Fig. 1. Nitrogen adsorption isotherms at −196 °C of AMS materials, prepared from silica sols with different molar HCl over TEOS ratio and *r*-value (cfr. Table 1).

The physical state of ibuprofen in the AMS materials was analyzed using DSC (Q-1000, TA Instruments, USA) in open aluminum sample pans. The samples were heated from −90 to 200 °C at 30 °C min^{-1}. Data were treated mathematically using the Universal Analysis 2000 software program (TA Instruments). The presence of a crystalline phase was verified using XRD on a Siemens D5000 instrument operated in reflection mode.

The concentration of the drug substance in the dissolution medium was determined using an isocratic HPLC method with UV detection. The HPLC system consisted of a Lachrom® L-7100 HPLC pump, an autosampler model L-7200, a UV detector model L-7420 set at 220 nm, and an Interface D-7000, all from Merck. UV signals were monitored and peaks were integrated using the D-7000 HSM software. All chromatographic separations were performed at room temperature. The analysis of ibuprofen was performed with a Merck Chromolith™ Performance RP-18e column. The mobile phase consisted of phosphate buffer (0.01 M, pH 5.5) and acetonitrile (Fisher Scientific, Tournai, Belgium) (60:40, v/v), filtered through a membrane filter (0.45 μm) and degassed by ultrasonication before use. The flow rate amounted to 1 ml min^{-1} and the injection volume was 10 μl.

3. Results and discussion

3.1. Tuning AMS microporosity

The following sol–gel synthesis parameters for AMS material synthesis were varied: the nature of the silicon alkoxide and solvent, the *r*-value (water over Si alkoxide molar ratio) and the HCl over Si molar ratio in the silica sol (Table 1). The solvent over Si alkoxide molar ratio was kept constant in this study. The texture of the AMS materials was characterized using nitrogen adsorption isotherms at −196 °C (Table 1 and Figs. 1 and 2). The HCl over Si molar ratio and *r*-value in the silica sol were varied between

Table 1
Code names of AMS materials according to the sol–gel synthesis parameters.

AMS material	Silicon alkoxide	Solvent	Solvent:Si molar ratio	HCl:Si molar ratio	*r*-Value	Micropore volume ($ml\,g^{-1}$)	BET surface area ($m^2\,g^{-1}$)
AMS1	TEOS	Ethanol	3	0.35	1.2	0.13	247
AMS2	TEOS	Ethanol	3	0.35	2	0.27	537
AMS3	TEOS	Ethanol	3	1.01	3.5	0.37	731
AMS4	TEOS	Ethanol	3	1.74	6	0.48	886
AMS5	TEOS	Ethanol	3	0.12	2	0.18	342
AMS6	TEOS	Ethanol	3	0.20	3.5	0.25	475
AMS7	TEOS	Ethanol	3	0.35	6	0.33	670
AMS8	TEOS	Methanol	3	0.35	2	0.26	517
AMS9	TMOS	Ethanol	3	0.35	2	0.22	424
AMS10	TMOS	Methanol	3	0.35	2	0.33	615

0.12–1.74 and 1.2–6, respectively (Table 1). The HCl over Si and *r*-value could not be varied independently because of the presence of water in concentrated HCl. AMS materials exhibit a type I isotherm typical of microporous materials (Figs. 1 and 2). AMS pore volume ranged from 0.13 to 0.48 $ml\,g^{-1}$. Such values of micropore volumes are typical of zeolite materials. The BET surface area of the different AMS samples was from 247 to 886 $m^2\,g^{-1}$ (Table 1).

Increasing the *r*-value from 1.2 to 2 under otherwise identical conditions (AMS1 and -2) resulted in a drastic increase in microporosity from 0.13 to 0.27 $ml\,g^{-1}$ (Table 1). In the AMS2-4 series, the *r*-value was increased from 2 to 6 and the HCl over Si ratio from 0.35 to 1.74. The increase of *r*-value to 6 and of the HCl over Si ratio to 1.74 led to an increase of the microporosity to 0.48 $ml\,g^{-1}$ for the AMS4 sample. Ultramicroporous materials with pore diameters smaller than 1.5 nm are characterized by a nitrogen adsorption isotherm that approaches maximum uptake at P/P_0 relative pressures below 0.1. Supermicroporous materials having micropores with diameters of 1.5–2.0 nm (Izquierdo-Barba et al., 2009) show nitrogen adsorption till relative pressures of 0.5. AMS1 and AMS5 were typical ultramicroporous materials, while AMS4 could be classified as a supermicroporous material (Fig. 1). AMS2, -3, -6 and -7 materials showed an intermediate behavior. The nitrogen adsorption isotherms illustrated in Fig. 1 demonstrates that an increase of the HCl to Si alkoxide ratio and *r*-value in the silica sol led to the formation of AMS materials with higher pore volumes and, based on the shape of the isotherm (Fig. 1), wider pore diameters. The micropore size distribution of AMS1–4 samples was determined using the Horvath–Kawazoe method (Horvath and Kawazoe, 1983), Fig. 3. All samples had a monomodal pore size distribution, with maxima around 3.6, 3.8, 4.2 and 4.5 å for AMS-1, -2, -3 and -4, respectively. The pore size distributions presented significant tailing to larger pore sizes (Fig. 3). The mean pore diameters were 4.0, 4.6, 5.1 and 5.4 å for AMS1, -2, -3 and -4, respectively.

Nitrogen adsorption isotherms of AMS materials prepared out of TEOS combined with methanol (AMS8) and from TMOS combined with ethanol and methanol (AMS9 and-10) are shown in Fig. 2. The molar HCl over Si alkoxide ratio and *r*-value were 0.35 and 2, respectively (Table 1). AMS materials prepared using TEOS and methanol (AMS8) and TMOS and ethanol (AMS9) combinations exhibited similar nitrogen adsorption isotherms and were classified as ultramicroporous materials, showing substantial nitrogen uptake only at very low relative pressures (Fig. 2). The material prepared from TMOS and methanol (AMS10) adsorbed nitrogen at relative pressures up to 0.5, and was classified as a supermicroporous material.

Table 2
Particle size distribution of AMS2 materials.[a].

AMS material	μ (μm)	σ (μm)	*A*
$AMS2_{80}$	80	–	–
$AMS2_{55}$	55	17	18
$AMS2_{220}$	216	56	22

[a] $AMS2_{55}$ and $AMS2_{220}$ were fitted by a Gaussian distribution function, with μ being the mean particle diameter and σ the standard deviation of the particle size distribution.

3.2. Particle fining

AMS material was manually fined using a mortar and pestle. The grinded powder was sieved. AMS1 and $AMS2_{80}$ powder was obtained using mesh size of 115, $AMS2_{55}$ was a combination of fractions obtained with mesh sizes 500 and 250. For separating the coarse sample $AMS2_{220}$ mesh sizes 60 and 65 were used and fractions combined. $AMS4_{800}$ resulted from a combination of mesh sizes 16 and 20. The particle size distribution and its fitting are reported in Fig. 4 and Table 2. $AMS2_{80}$ fined in a mortar had a broad particle size distribution, with a mean diameter of 80 μm and a 75% confidence range from 30 to 225 μm (Fig. 4a). Fractions obtained by sieving, denoted $AMS2_{55}$ and $AMS2_{220}$ displayed a normal size distribution and could be fitted by a Gaussian distribution function (Fig. 4b and c, Table 2).

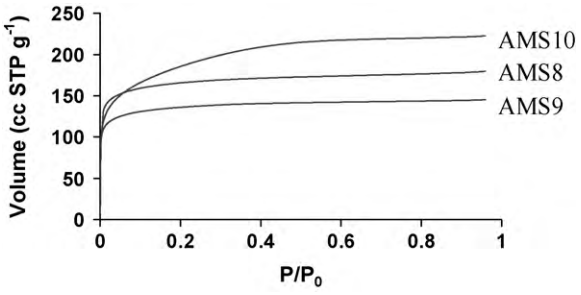

Fig. 2. Nitrogen adsorption isotherms at −196 °C of AMS materials, prepared from different alkoxide sources and solvents (Table 1).

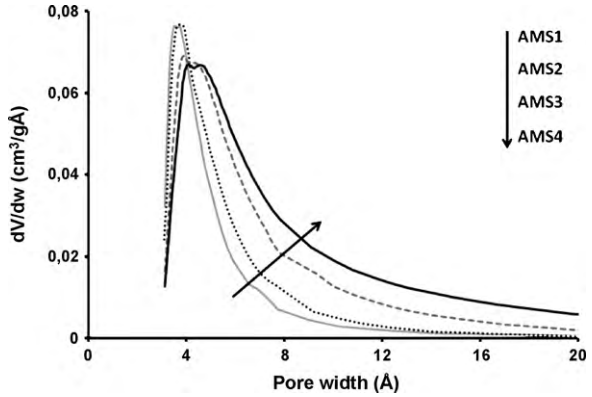

Fig. 3. Micropore size distribution of AMS1, AMS2, AMS3 and AMS4.

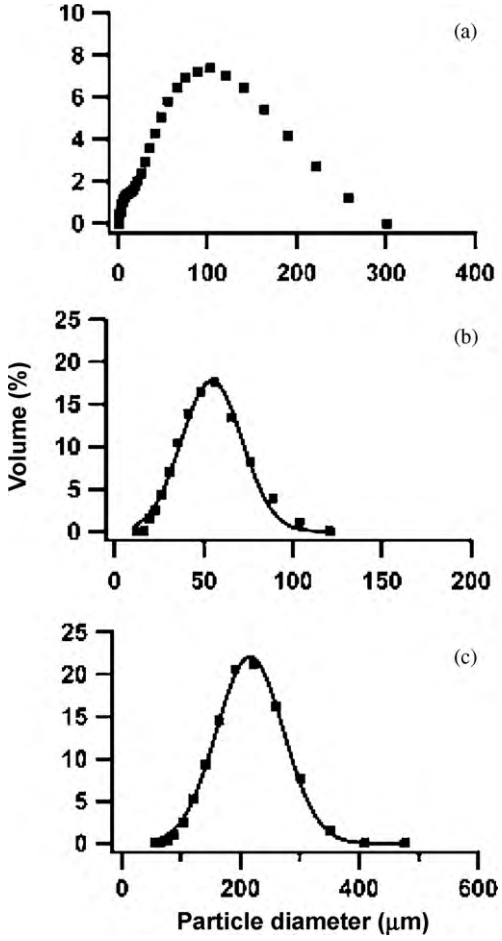

Fig. 4. Particle size distribution of $AMS2_{80}$ (a), $AMS2_{55}$ (b) and $AMS2_{220}$ (c). The distribution of $AMS2_{55}$ and $AMS2_{220}$ was fitted by a Gaussian distribution curve (Table 2).

3.3. In vitro release experiments

$AMS1_{80}$, $AMS2_{80}$, $AMS2_{220}$ and $AMS2_{55}$ powders were loaded with 10 wt.% ibuprofen by heating physical mixtures above the melting point of ibuprofen. From the absence of DSC signals ascribed to crystalline and glassy ibuprofen it was concluded that ibuprofen was molecularly dispersed in the AMS2 samples (Fig. 5) (Aerts et al., 2007), while the result for loaded $AMS1_{80}$ displays a clear melting peak of crystalline ibuprofen. XRD diagrams of 10 wt.% loaded $AMS1_{80}$ sample (Fig. 6) displayed sharp diffraction peaks caused by the presence of crystalline ibuprofen. The XRD signature of crystalline ibuprofen was absent in the $AMS2_{80}$ sample. Ibuprofen release from the AMS2 materials was analyzed in a dissolution medium simulating the transition from acidic to neutral environment in the human gastrointestinal tract (Fig. 7). During the first two hours, the release medium was simulated gastric fluid (SGF, pH 1.2); after 2 h, the pH was raised to 6.8 by adding K_2HPO_4, resulting in a medium simulating human intestinal fluid (SIF).

The ibuprofen release kinetics from AMS2 were strongly influenced by milling (Fig. 7): the smaller the particles, the more rapid the release. $AMS2_{80}$ had a broad particle size distribution (Fig. 4a). At pH 1.2, an ibuprofen release of 25% was reached after one and a half hour. Upon changing the pH to 6.8, the ibuprofen release jumped to ca. 40%, followed by a period of slower release. The solubility of the ibuprofen molecule in acidic environment of SGF is low and estimated at 31 mg l^{-1}. At 25% release, the concentration of ibuprofen in the release medium was about 10% of the determined maximal solubility in SGF. The slowing of the ibuprofen release after 25% release may be due to several reasons. Possibly in the first hour ibuprofen had been released from the largest pores. Alternatively, there may have been local supersaturation in the fluid film around the particles, causing precipitation blocking the pores. The sudden increase of the release upon switching from acidic to neutral pH can be explained by the much better solubility of ibuprofen in SIF medium, amounting to 4.4 g l^{-1}. Ibuprofen release from $AMS2_{80}$ lasted several hours. After 8 h, the cumulative release amounted to 82% (Fig. 7a). The presence of a fraction of large particles was responsible for the sustained release. In contrast to $AMS2_{80}$ materials, $AMS2_{220}$ did not contain a significant amount of fine AMS powder (Fig. 4c). In acidic medium as well as neutral medium there was sustained release. There was a minor jump in the cumulative ibuprofen release curve upon changing the pH. The ibuprofen precipitation phenomenon inferred for the $AMS2_{80}$ material was almost absent. Cumulative ibuprofen release from $AMS2_{220}$ was 30% after 4 h and 62% after 8 h (Fig. 7a).

$AMS2_{55}$ material representing a fine fraction obtained by sieving of AMS2 manually grinded with the mortar had a narrow particle size distribution (Fig. 4b). Ibuprofen release from $AMS2_{55}$ particles

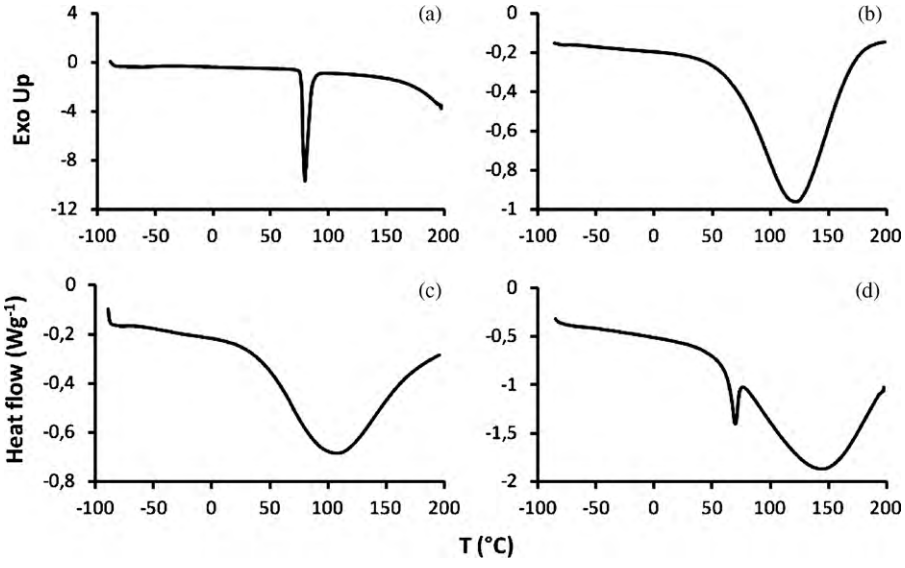

Fig. 5. DSC thermograms of pure ibuprofen (a), $AMS2_{80}$ (b), 10 wt.% loaded $AMS2_{80}$ (c) and 10 wt.% loaded $AMS1_{80}$ (d).

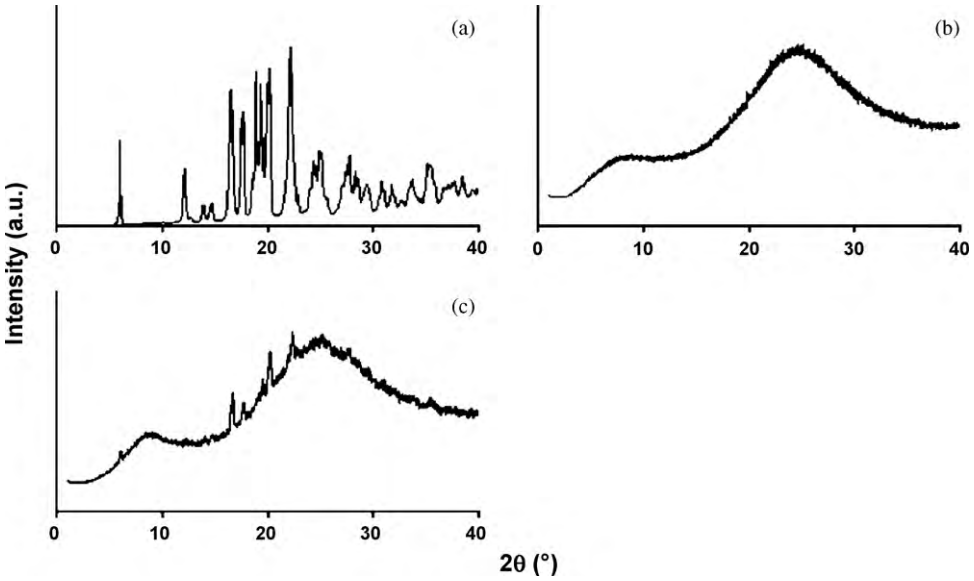

Fig. 6. XRD patterns for pure ibuprofen (a), 10 wt.% loaded $AMS2_{80}$ (b) and 10 wt.% loaded $AMS1_{80}$ (c).

in acidic medium was very fast. Again, the release reached a plateau due to the rather limited solubility in the acidic medium. Immediately after the transition from acidic to neutral environment, the cumulative ibuprofen release approached 100% (Fig. 7b). The particles of $AMS2_{55}$ sample seemingly are too small for realizing a sustained release.

3.4. Stability study

In aqueous environment porous amorphous silica materials tend to be unstable. It is well documented that the stability in water of ordered mesoporous materials is critically dependent on the silica wall thickness (Zhao et al., 1998; Frias et al., 2001).

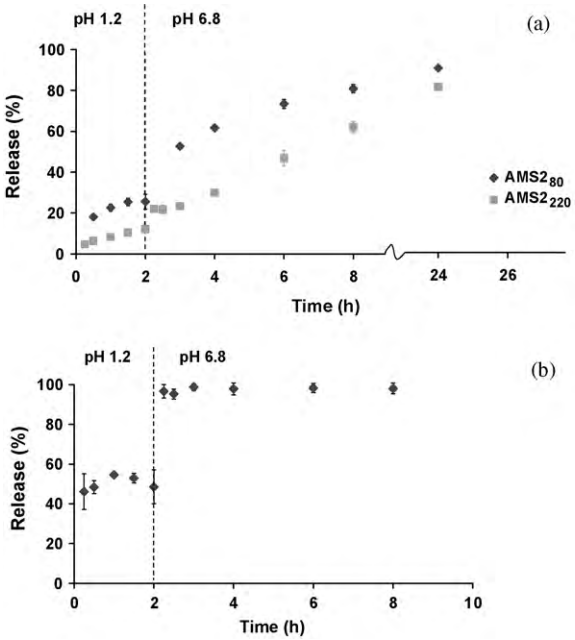

Fig. 7. Ibuprofen release from AMS/ibuprofen formulations in a dissolution medium simulating the gastrointestinal tract. (a) $AMS2_{80}$ and $AMS2_{220}$ ($n = 3$), (b) $AMS2_{55}$ ($n = 2$). The AMS materials were loaded with 10 wt.% ibuprofen by the melting method.

Therefore, we explored the stability of AMS in different media. $AMS2_{80}$ materials were dispersed in ethanol, methylene chloride, simulated intestinal fluid (SIF, pH 6.8) and simulated gastric fluid (SGF, pH 1.2). After 2 h, the powders were filtered, washed and dried at 40 °C during 48 h. When $AMS2_{80}$ was dispersed in ethanol or methylene chloride and dried again, no decrease in micropore volume was observed. The pore structure of $AMS2_{80}$ was less stable in aqueous suspension (Fig. 8). The micropore volume of $AMS2_{80}$ decreased by 54% after dispersion in SIF during 2 h. The decrease in porosity was less pronounced (only 18%) after dispersion of $AMS2_{80}$ in the acidic SGF medium. Silica is known to be more stable at low pH where its solubility is lower.

AMS4, prepared from a silica sol with higher water content in comparison to AMS2 (Table 1), was more robust. After dispersion in SIF during 24 h, the micropore volume of $AMS4_{800}$ had decreased by only 9%.

The stability of dry AMS materials under ambient storage conditions was investigated by analyzing the evolution of the porosity of the samples with time using nitrogen physisorption. This study revealed that the stability of the AMS pore structure was influenced by the particle size. Fig. 9 shows the nitrogen adsorption isotherms of coarse AMS2 grains of millimeter size and AMS2 powder particles milled in a mortar to a mean size of ca. 80 μm ($AMS2_{80}$). The isotherms were recorded immediately after synthesis of the materials and after storage under ambient conditions over 6 months.

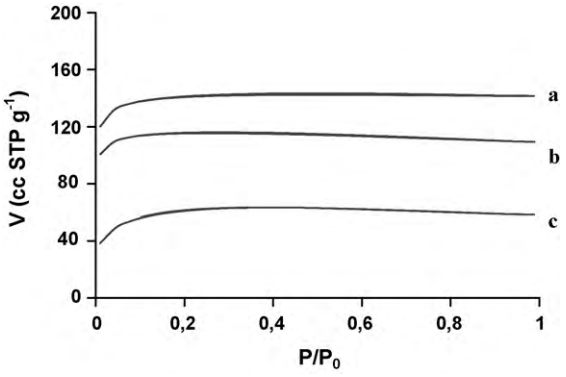

Fig. 8. Nitrogen adsorption isotherms of $AMS2_{80}$ materials: parent material (a), after dispersion in SGF during 2 h (b) and after dispersion in SIF during 2 h (c).

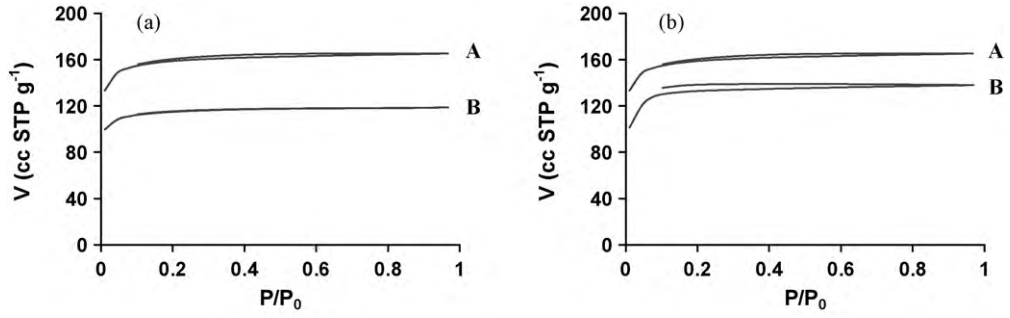

Fig. 9. Nitrogen adsorption and desorption isotherms of AMS2 materials immediately after synthesis (A) and after storage during 6 months under ambient conditions (B): (a) $AMS2_{80}$ powder, (b) coarse AMS2 grains of millimeter size.

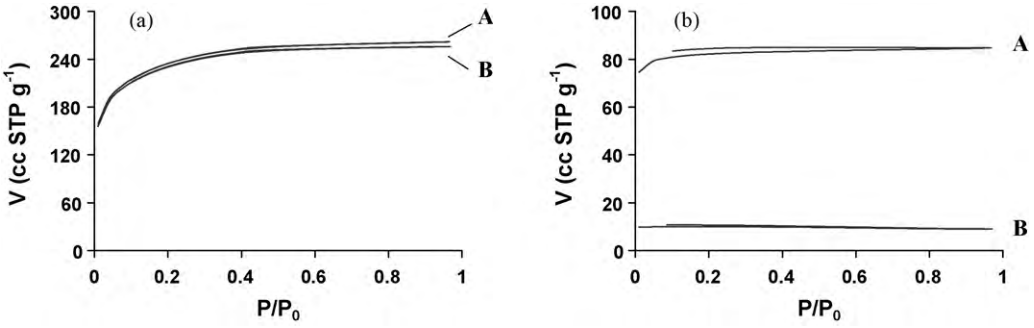

Fig. 10. Nitrogen adsorption isotherms of AMS materials immediately after synthesis (A) and after storage during 5 months under ambient conditions (B): (a) coarse AMS3 grains of millimeter size, (b) coarse AMS1 grains of millimeter size.

The micropore volume of coarse AMS2 grains and $AMS2_{80}$ powder decreased by about 16% and 28%, respectively, over a period of 6 months. The values reveal that small AMS particles are most sensitive to degradation.

The AMS stability was also dependent on the sol–gel synthesis parameters. The pore structure of AMS3, prepared from a silica sol with a higher acid and water content in comparison to AMS2 (cfr. Table 1), was more stable. The porosity of AMS3 particles of millimeter size was still intact after storage over 5 months (Fig. 10a). In contrast, the AMS1 sample prepared using a lower water content (cfr. Table 1) was rather unstable. The pore volume had decreased by about 85% over 5 months of storage (Fig. 10b). These results reveal that AMS stability is significantly improved when large amounts of water are used in the synthesis. Apparently, the higher water content results in a higher degree of hydrolysis and condensation, which leads to the formation of more condensed and more rigid structures.

The AMS stability also depends on the silicon alkoxide and solvent source used in the synthesis. AMS materials prepared from TEOS and methanol (AMS8) and TMOS and ethanol (AMS9) show a stability similar to that of AMS2 materials, prepared from TEOS and ethanol under otherwise identical conditions (cfr. Table 1). AMS material synthesized from TMOS and methanol (AMS10) was more stable and retained its microporosity over a period of 4 months at least.

Stability studies of ibuprofen loaded $AMS2_{80}$ formulations were performed. $AMS2_{80}$ materials, loaded with 10 wt.% ibuprofen by impregnation, were stored in a small polypropylene bottle over 6 months under ambient conditions and over 1 year at 25 °C at a relative humidity of 0%. Immediately after drug loading, $AMS2_{80}$ was analyzed using DSC in order to verify the physical state of ibuprofen in the formulation. The absence of DSC signals ascribed to crystalline and glassy ibuprofen suggest that ibuprofen was in a molecularly dispersed state. After storage under ambient conditions over 6 months, DSC analysis revealed a melting peak of ibuprofen, representing 5% of the total drug content (Fig. 11a). The presence of some crystalline ibuprofen can be tentatively explained by the crystallization of ibuprofen molecules that were located on the outer surface of the silica particles where there was sufficient space for nucleation and crystal growth. Ibuprofen release was analyzed in a dissolution medium simulating the transition from acidic to neutral environment in the human gastrointestinal

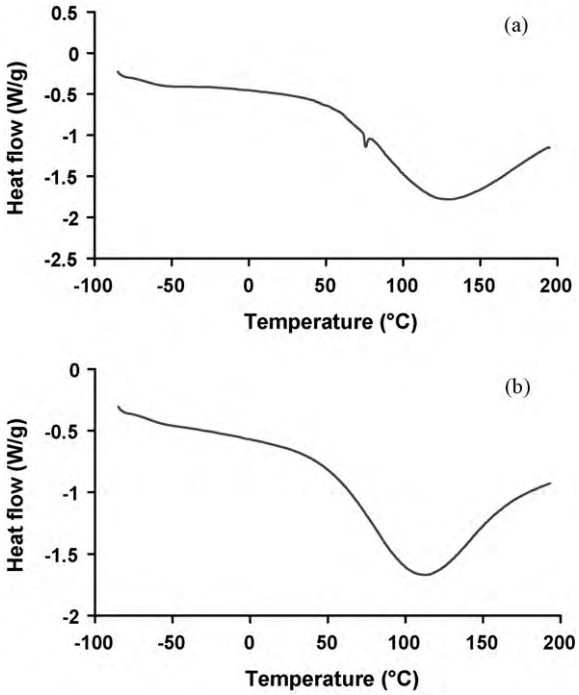

Fig. 11. DSC analysis of ibuprofen loaded (10 wt.%) $AMS2_{80}$: (a) after storage during 6 months at ambient conditions, (b) after storage during 1 year at 25 °C and at a relative humidity of 0%.

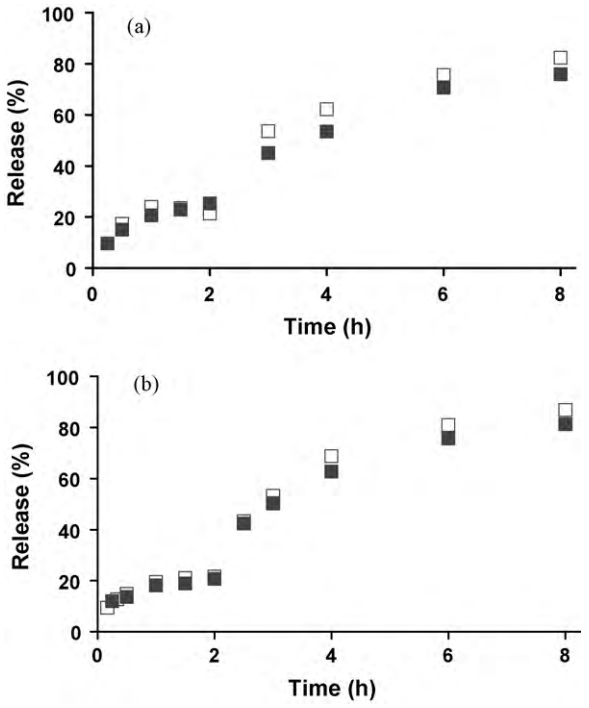

Fig. 12. (a) Ibuprofen release from a freshly prepared $AMS2_{80}$ formulation (□) and after 6 months storage under ambient conditions (■), (b) ibuprofen release from a freshly prepared $AMS2_{80}$ formulation (□) and after storage during 1 year at 25 °C and at a relative humidity of 0% (■). $AMS2_{80}$ was loaded with 10 wt.% ibuprofen using the impregnation method.

tract (Fig. 12a). After 8 h, cumulative ibuprofen release from the freshly prepared formulation and the aged sample was 82% and 76%, respectively. Ibuprofen release kinetics were hardly changed after storage under ambient conditions for 6 months. Apparently, drug release was not influenced by the small fraction of crystalline ibuprofen in the formulation after storage detected by DSC. Ibuprofen molecules on the external surface of the AMS carrier irrespective of their state are rapidly released after contact with the dissolution medium. The pore structure of unloaded AMS2 was shown to degrade upon storage over months (cfr. Fig. 9). The unaffected pharmaceutical performance of loaded AMS formulations (Fig. 12a) can be attributed to the presence of ibuprofen molecules in the pores, functioning as stabilizing agents of the pore structure.

Additionally, ibuprofen loaded $AMS2_{80}$ was stored during 1 year at 25 °C and at a relative humidity of 0%. The dissolution profile of a freshly prepared $AMS2_{80}$ formulation and an aged sample is compared in Fig. 12b. No remarkable changes in release kinetics could be observed. After 8 h, the cumulative ibuprofen release was 86% and 81%, respectively. DSC analysis revealed that ibuprofen loaded $AMS2_{80}$, stored during 1 year in dry atmosphere, was stable. No thermal transitions of ibuprofen could be observed in the thermogram of this sample (Fig. 11b). Apparently, no crystallization of the drug substance occurred when contact with water molecules was avoided during storage.

4. Conclusions

The porosity of AMS can be adapted by varying several sol–gel synthesis parameters including the molar hydrolysis ratio (*r*-value), HCl:Si molar ratio, the type of silicon alkoxide source and the solvent. The micropore volume available for drug loading ranged from 0.13 to 0.48 ml g^{-1}. *In vitro* release experiments demonstrated that the particle size and the width of the particle size distribution of the AMS2 carrier material affect the diffusion controlled ibuprofen release profile.

Stability studies on unloaded AMS materials revealed a loss of porosity upon storage under ambient conditions. The decrease in porosity can be attributed to a sintering process catalyzed by water molecules from the atmosphere. Small AMS particles are most sensitive to this degradation process. The AMS stability is dependent on synthesis procedure. Materials synthesized from silica sol with high water content are most stable. Ibuprofen loaded AMS2 formulations show excellent stability upon long term storage. Ibuprofen molecules in the pores seem to support the pore structure.

Acknowledgments

C.A.A. acknowledges the Institute for the Promotion of Innovation through Science and Technology in Flanders (IWT Vlaanderen) for a research fellowship. R.M. acknowledges the Flemish FWO for a post-doctoral fellowship. The work was supported by a K.U. Leuven interdisciplinary research project (IDO) and an industrial research fund (IOF). J.A.M. acknowledges the Flemish government for long-term structural funding (Methusalem).

References

Aerts, C.A., Verraedt, E., Mellaerts, R., Depla, A., Augustijns, P., Van Humbeeck, J., Van den Mooter, G., Martens, J.A., 2007. Tunability of pore diameter and particle size of amorphous microporous silica for diffusive controlled release of drug compounds. J. Phys. Chem. C 111, 13404–13409.
Ahola, M., Kortesuo, P., Kangasniemi, I., Kiesvaara, J., Yli-Urpo, A., 2000. Silica xerogel carrier material for controlled release of toremifene citrate. Int. J. Pharm. 195, 219–227.
Ahola, M.S., Säilynoja, E.S., Raitavuo, M.H., Vaahtio, M.M., Salonen, J.I., Yli-Urpo, A.U.O., 2001. In vitro release of heparin from silica xerogels. Biomaterials 22, 2163–2170.
Angelos, S., Johanson, E., Stoddart, J.F., Zink, J.I., 2007. Mesostructured silica supports for functional materials and molecular machines. Adv. Funct. Mater. 17, 2261–2271.
Brinker, C.J., 1988. Hydrolysis and condensation of silicates: effects on structure. J. Non-Cryst. Solids 100, 31–50.
Brinker, C., Scherer, G., 1990. Sol–Gel Science: The Physics and Chemistry of Sol–Gel Processing. Academic Press Inc., San Diego.
Charnay, C., Bégu, S., Tourné-Péteilh, C., Nicole, L., Lerner, D.A., Devoisselle, J.M., 2004. Inclusion of ibuprofen in mesoporous templated silica: drug loading and release property. Eur. J. Pharm. Biopharm. 57, 533–540.
Czuryszkiewicz, T., Ahvenlammi, J., Kortesuo, P., Ahola, M., Kleitz, F., Jokinen, M., Lindén, M., Rosenholm, J.B., 2002. Drug release from biodegradable silica fibers. J. Non-Cryst. Solids 306, 1–10.
Deng, Y., Lettmann, C., Maier, W.F., 2001. Leaching of amorphous V- and Ti-containing porous silica catalysts in liquid phase oxidation reactions. Appl. Catal. A 214, 31–46.
Doadrio, A.L., Sousa, E.M.B., Doadrio, J.C., Perez-Pariente, J., Izquierdo-Barba, I., Vallet-Regi, M., 2004. Mesoporous SBA-15 HPLC evaluation for controlled gentamicin drug delivery. J. Control. Release 97, 125–132.
Frenzer, G., Maier, W.F., 2006. Amorphous porous mixed oxides: sol–gel ways to a highly versatile class of materials and catalysts. Annu. Rev. Mater. Res. 36, 281–331.
Frias, J., Olle, E., Alsina, M., 2001. Periodontal pathogens produce quorum sensing signal molecules. Infect. Immun. 69, 3431–3434.
Grimm, J., Bessarabov, D., Maier, W., Storck, S., Sanderson, R.D., 1998. Sol-gel film-preparation of novel electrodes for the electrocatalytic oxidation of organic pollutants in water. Desalination 115, 295–302.
Heikkila, T., Salonen, J., Tuura, J., Hamdy, M.S., Mul, G., Kumar, N., Salmi, T., Murzin, D.Y., Laitinen, L., Kaukonen, A.M., Hirvonen, J., Lehto, V.P., 2007. Mesoporous silica material TUD-1 as a drug delivery system. Int. J. Pharm. 331, 133–138.
Horcajada, P., Ramila, A., Perez-Pariente, J., Vallet-Regi, M., 2004. Influence of pore size of MCM-41 matrices on drug delivery rate. Micropor. Mesopor. Mater. 68, 105–109.
Horcajada, P., Marquez-Alvarez, C., Ramila, A., Pérez-Pariente, J., Vallet-Regi, M., 2006a. Controlled release of ibuprofen from dealuminated faujasites. Solid State Sci. 8, 1459–1465.
Horcajada, P., Ramila, A., Ferey, G., Vallet-Regi, M., 2006b. Influence of superficial organic modification of MCM-41 matrices on drug delivery rate. Solid State Sci. 8, 1243–1249.
Horvath, G., Kawazoe, K., 1983. Method for the calculation of effective pore-size distribution in molecular-sieve carbon. J. Chem. Eng. Jpn. 16, 470–475.
Izquierdo-Barba, I., Martinez, F., Doadrio, A.L., Pérez-Pariente, J., Vallet-Regi, M., 2005. Release evaluation of drugs from ordered three-dimensional silica structures. Eur. J. Pharm. Biopharm. 26, 365–373.

Izquierdo-Barba, I., Vallet-Regi, M., Kupferschmidt, N., Terasaki, O., Schmidtchen, A., Malmsten, M., 2009. Incorporation of antimicrobial compounds in mesoporous silica film monolith. Biomaterials 30, 5729–5736.

Konietzni, F., Zanthoff, H.W., Maier, W.F., 1999. The role of active oxygen in the AMM-VxSi-catalysed selective oxidation of toluene. J. Catal. 188, 154–164.

Konietzni, F., Kolb, U., Dingerdissen, U., Maier, W.F., 1998. AMM-MnxSi-catalyzed selective oxidation of toluene. J. Catal. 176, 527–535.

Kortesuo, P., Ahola, M., Karlsson, S., Kangasniemi, I., Yli-Urpo, A., 1999. Sol–gel processed sintered silica xerogel as a carrier in controlled drug delivery. J. Biomed. Mater. Res. 44, 162–167.

Kortesuo, P., Ahola, M., Kangas, M., Kangasniemi, I., Yli-Urpo, A., Kiesvaara, J., 2000a. In vitro evaluation of sol–gel processed spray dried silica gel microspheres as carrier in controlled drug delivery. Int. J. Pharm. 200, 223–229.

Kortesuo, P., Ahola, M., Kangas, M., Leino, T., Laakso, S., Vuorilehto, L., Yli-Urpo, A., Kiesvaara, J., Marvola, M., 2001a. Alkyl-substituted silica gel as a carrier in the controlled release of dexmedetomidine. J. Control. Release 76, 227–238.

Kortesuo, P., Ahola, M., Kangas, M., Yli-Urpo, A., Kiesvaara, J., Marvola, M., 2001b. In vitro release of dexmedetomidine from silica xerogel monoliths: effect of sol–gel synthesis parameters. Int. J. Pharm. 221, 107–114.

Kortesuo, P., Ahola, M., Karlsson, S., Kangasniemi, I., Yli-Urpo, A., Kiesvaara, J., 2000b. Silica xerogel as an implantable carrier for controlled drug delivery: evaluation of drug distribution and tissue effects after implantation. Biomaterials 21, 193–198.

Lai, C.Y., Trewyn, B.G., Jeftinija, D.M., Jeftinija, K., Xu, S., Jeftinija, S., Lin, V.S., 2003. A mesoporous silica nanosphere-based carrier system with chemically removable CdS nanoparticle caps for stimuli-responsive controlled release of neurotransmitters and drug molecules. J. Am. Chem. Soc. 125, 4451–4459.

Li, W., Lettmann, C., Maier, W., 2000. Amorphous porous MxTi mixed oxides as catalysts for the oxidative dehydrogenation of ethylbenzene. Catal. Lett. 69, 181–188.

Maier, W.F., Tilgner, I.-C., Wiedorn, M., Ko, H.-C., 1993. Preparation and characterization of microporous metal oxides. Adv. Mater. 5, 726–730.

Mellaerts, R., Aerts, C.A., Van Humbeeck, J., Augustijns, P., Van den Mooter, G., Martens, J.A., 2007. Enhanced release of itraconazole from ordered mesoporous SBA-15 silica materials. Chem. Commun. 13, 1375–1377.

Munoz, B., Ramila, A., Perez-Pariente, J., Diaz, I., Vallet-Regi, M., 2002. MCM-41 organic modification as drug delivery rate regulator. Chem. Mater. 15, 500–503.

Oresek, H., Schulz, R., Dingerdissen, U., Maier, W., 1999. Selective oxidation of propene with air to propylene oxide, a case study of autooxidation versus catalytic oxidation with AMM-catalysts. Chem. Eng. Technol. 22, 691–700.

Ro, J.C., In, J.C., 1991. Structures and properties of silica gels prepared by the sol–gel method. J. Non-Cryst. Solids 130, 8–17.

Santos, E.M., Radin, S., Ducheyne, P., 1999. Sol–gel derived carrier for the controlled release of proteins. Biomaterials 20, 1695–1700.

Stöckmann, M., Konietzni, F., Notheis, J.U., Voss, J., Keune, W., Maier, W.F., 2001. Selective oxidation of benzene to phenol in the liquid phase with amorphous microporous mixed oxides. Appl. Catal. A 208, 343–358.

Storck, S., Maier, W.F., Miranda Salvado, I.M., Ferreira, J.M.F., Guhl, D., Souverijns, W., Martens, J.A., 1997. Amorphous Sn/Si mixed oxides, mild solid Lewis acid catalysts for esterification and etherification reactions. J. Catal. 172, 414–426.

Vallet-Regi, M., Ramila, A., del Real, R.P., Perez-Pariente, J., 2000. A new property of MCM-41: drug delivery system. Chem. Mater. 13, 308–311.

Verraedt, E., Pendela, M., Adams, E., Hoogmartens, J., Martens, J.A., 2010. Controlled release of chlorhexidine from amorphous microporous silica. J. Control. Release 142, 47–52.

Zeng, W., Qian, X.F., Zhang, Y.B., Yin, J., Zhu, Z.K., 2005. Organic modified mesoporous MCM-41 through solvothermal process as drug delivery system. Mater. Res. Bull. 40, 766–772.

Zhao, D., Feng, J., Huo, Q., Melosh, N., Fredrickson, G.H., Chmelka, B.F., Stucky, G.D., 1998. Triblock copolymer syntheses of mesoporous silica with periodic 50 to 300 Angstrom pores. Science 279, 548–552.